Multimedia Tools and Applications (2020) 79:10629–10638
https://doi.org/10.1007/s11042-019-7616-2

On the crack evolution and failure form of concrete specimens based on minimum energy principle

Xinyu Liang[1]

Received: 23 February 2019 / Revised: 23 March 2019 / Accepted: 8 April 2019 /
Published online: 1 May 2019

Abstract
By subjecting concrete specimens to pressure and tension under different loading conditions, this paper studies the relationships of stress state with crack opening and development and failure forms of specimens. Based on the principle of conservation of energy, it explores the relationship between failure area, failure energy and strength. The numerical calculation and CT test results show that the stress state of concrete determines the failure form, that the failure form determines the failure area, that failure area determines the energy consumed by the failure and that the failure energy determines the strength of the specimen, regardless of how the specimen is loaded.

Keywords Concrete · CT test · Stress state · Failure area · Failure energy

1 Introduction

The strength of concrete is an intrinsic property of this material and a mechanical quantity that does not vary with the external conditions. The Italian scientist Galilei first proposed the maximum normal stress theory in l638 in the book Two New Sciences, which was later revised as the maximum tensile stress theory. As the earliest proposed strength theory, it considers only one of the three principal stresses, which is not reasonable enough. The French Scientist E. Mariotte proposed the maximum linear strain theory in 1682, which was later revised as the theory of maximum elongation strain, but it is inconsistent with the experimental results of most materials; the French scientist C.A. Coulomb proposed the maximum shear stress theory in 1773, which only applies to materials of equal tensile and compressive strength. The Italian Scientist *E. Beltrami* proposed the energy theory in 1885, which was subsequently revised by M.T. Huber in 1904 as the maximum distortion energy theory.

It is known that the tensile, compressive, shear, torsional and flexural strengths of the same concrete specimen are different, and that the static and dynamic tensile and compressive

✉ Xinyu Liang
key_xinyu@163.com

[1] School of Civil Engineering & Architecture, Xi'an Technological University, Xian, China

strengths also increase at different rates; and under the same load, when the height, effective sectional area and section shape change, the measured strength also changes. Do these differences arise from the definition of concrete strength, the test method or a more complicated reason? There are many studies regarding this at home and abroad [1–6, 9–14, 16].

This paper studies the relationship between the failure form and the strength of concrete specimens from the perspective of crack energy release rate through CT test and numerical test.

2 Study of the crack evolution mechanism of concrete specimens under static tensile and compressive loads through CT tests

The static tension and compression CT tests on concrete specimens were carried out with the portable material dynamic testing machine developed by Xi'an University of Technology [7, 8, 15, 17] in the CT room at Affiliated Renhe Hospital of China Three Gorges University.

2.1 Specimen preparation

The concrete strength was C15 and the water-cement ratio 0.50. The cement used was the 42.5 moderate heat Portland cement produced in Yunnan Dianxi Cement Plant; the aggregate consists of natural gravel aggregate and natural sand from the aggregate field of Bandu Hydropower Station. The specimens are cylinders with a height of 120 mm and a diameter of 60 mm, with the coarse aggregate size being no more than 10 mm. The representative specimens are tension specimen conc-004 and compression specimen conc-066.

The failure form and surface of conc-004 are shown in Figs. 1 and 2. Under the static tensile stress, crack initiation can hardly be captured in CT images, as the tensile strength of concrete material is very low and the concrete specimen would quickly break along its cross section under tension. Once the crack is initiated, it will rapidly expand along the cross section (vertical to the loading direction). During loading, the breaking process is very short and sudden.

The failure form and surface of conc-066 are shown in Fig. 3. Under the static tensile stress, cracks are mostly vertically distributed and well developed. The failure surface resulting from crack coalescence is cone-shaped and usually the cracks would not penetrate through the aggregate. After the main crack is formed, the specimen would still have some residual

Fig. 1 Specimen conc-004

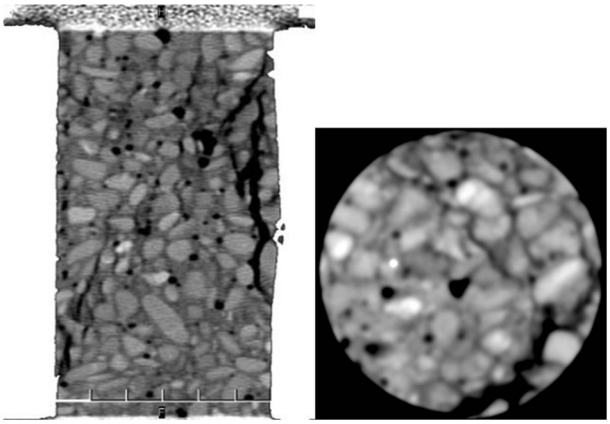

Fig. 2 Tensile failure surface of conc-004

strength. It takes a very long time from crack formation to the failure of the whole specimen. Static failure shows very obvious signs of softening and forms mode II shear cracks.

2.2 Analysis of the cracks and failure surfaces of concrete specimens through CT test

The area of the failure surface of the specimen is equal to the number of cells in the crack zone multiplied by the area per resolution cell. In this experiment, a = 0.35 mm and b = 0.49 mm. According to the CT-image-based crack calculation theory, based on experimental observations, the average change in the CT number of the statistical zone was caused by the average change in the CT number in the crack zone after the crack occurred, that is, the change in the average CT number in S0 was equal to the change in the average CT number in SD:

$$S_{\mathrm{D}} = \frac{H_0 - H_i}{1000 + H_i} S_0 \tag{1}$$

H0 and Hi are the CT number at each point or specific statistic zone at the initial stress stage and some other stress stage, respectively; S0 is the area of the statistical zone before the crack appears; SD is the failure area.

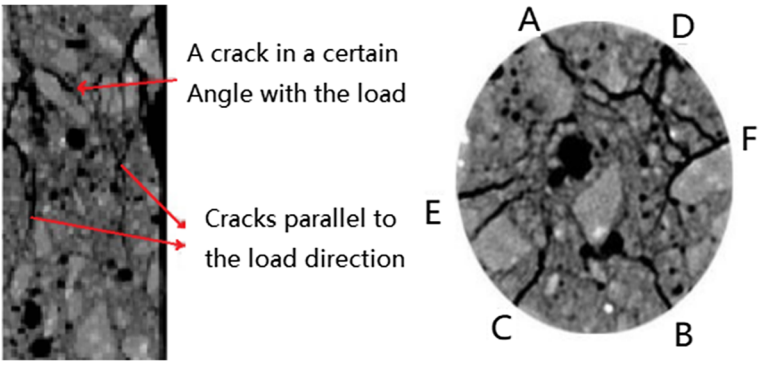

Fig. 3 Compressive failure surface of conc-066

Through CT tests, it was found that the failure area of the tension specimen was smaller than that of the compression specimen and that the failure energy of the tension specimen was also smaller than that of the compression one.

In the process of loading, due to the different crack initiation and development paths and different crack evolution patterns, if the failure area of the compression specimen was far larger than that of the tension one and the failure energy of the compression specimen far greater than that of the tension one, then the strength of the compression specimen was also far greater than that of the tension one. This was mainly caused by the different stress distributions inside the concrete materials under tension and shear compression. Under the static compressive stress, there were many cracks. Cracks initiation and penetration required a lot of energy, and a great amount of energy was also release later, gradually forming failure surfaces in the 3D concrete specimen. Under the static tensile stress, the failure surface was relatively flat and cracks mostly appeared along the mortar and the cement plane between the mortar and the aggregate. The crack formation required less energy. On the contrary, under static compression, there were many complex cracks, and the failure surfaces were varied. Subsequently, a lot of additional damage energy was released. The amount of energy released from crack initiation, development and penetration was closely related to the crack development direction and depended on the stress condition of the specimen.

2.3 Study of the crack development of load-bearing concrete specimens

A bilinear damage evolution model is adopted for numerical simulation.In this paper, a bilinear damage evolution model is adopted for numerical simulation, which can simulate the initiation, development and penetration of cracks in concrete specimens, and simulate the process of gradual failure of materials through elastic damage model.

2.3.1 Pull-1 model

From the numerical simulation shown in Fig. 4, it can be seen that, when the concrete specimen was tensioned, the stress at the tip of the crack perpendicular to the tensile stress tended to concentrate and that the crack began to expand along the tip and kept developing in the plane of the crack. As the crack expanded, the stress around it was also getting more concentrated, leading to unstable crack development. It extended to the edge of the concrete specimen until the specimen ruptured. Therefore, the cracks were transversely distributed and perpendicular to the direction of the tensile stress. They developed along the main crack until the failure occurred. The failure surface is located along the cross section of the specimen.

2.3.2 PRE-1 concrete specimen under compression

As shown in Fig. 5, the failure surface of the concrete specimen under compression was at an angle to the horizontal plane instead of being along the longitudinal section of the specimen. Through analysis, it was found to be a shear failure, as the crack penetration surface, i.e. the failure surface. Was oval, which was a shear failure surface. In the diagram of the damaged interface, the cracking form looked like a "×".

In Figs. 4 and 5 The white part in the figure represents the crack generated in the process of stress on the specimen. In the numerical simulation, the elastic modulus of the element

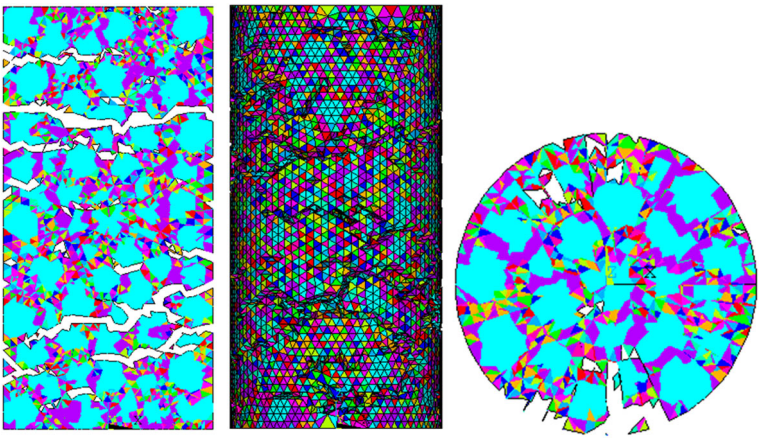

Fig. 4 Pull-1 damaged cells

gradually decreases with the difference of damage variables. When the damage variable of some elements is 1, the element will fail.

3 Study of the failure process of loading-bearing concrete specimens

For the concrete specimen under tension loaded in the displacement-control mode, as shown in Fig. 6, with the tensile force increasing, before it reached 10.62kN, the displacement showed linear elastic variations, and with the further increase of the tensile force, the elasticity modulus was damaged, and the slopes of the tension and displacement curves became smaller. When the tensile force reached 15.47kN, with the displacement increasing, the tensile force greatly decreased, and some of the cells in the concrete specimen were damaged. At this point, the tensile force of the specimen reached the maximum, the corresponding stress was the maximum stress

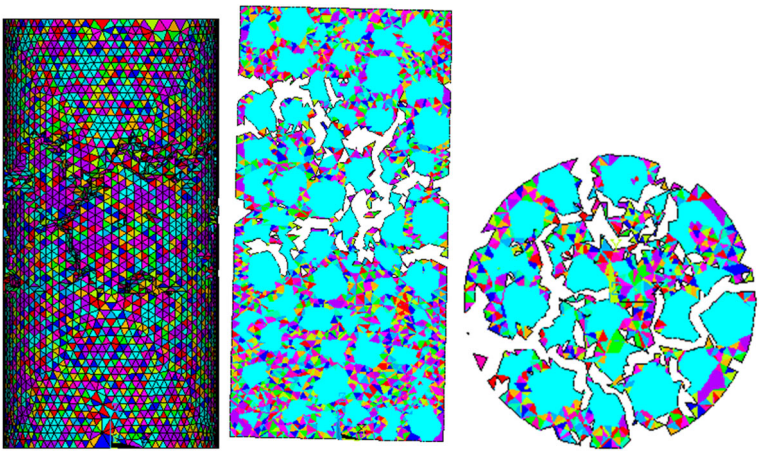

Fig. 5 PRE-1 damages and damaged interface

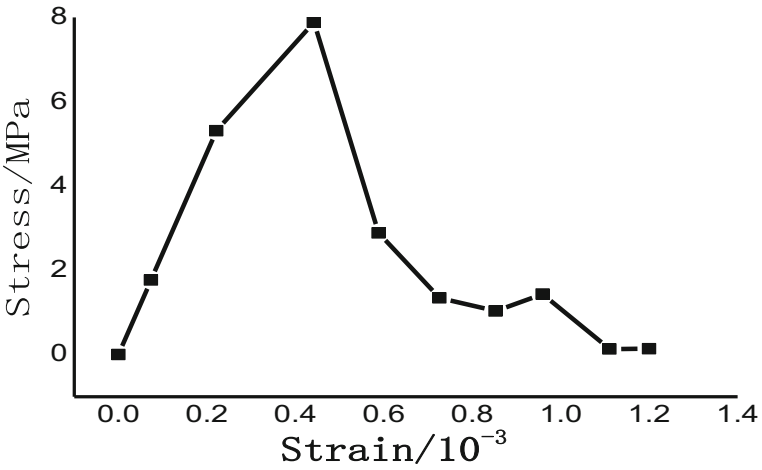

Fig. 6 Pull-1 stress-strain curve

value and the strength failed. As the displacement continued to increase, the tensile force decreased until the load did not converge, which was when the concrete specimen failed.

Before the stress reached 5.31 MPa, the stress changed linearly with the strain, but after that, the slope of the stress curve with the strain decreased, part of the cells in the interface and the mortar were damaged and the elastic modulus was damaged and attenuated. Microcracks appeared in the specimen and the cracks inside the specimen expanded in a rapid and unstable manner. When the stress reached 7.88 MPa, which was the maximum value, the strain gradually increased. As the cracks in the specimen gradually converged and formed into a large crack, the stress decreased rapidly. At this point, part of the cells was damaged, and the strength of the specimen started to fail. The strain continued to increase, and the stress decreased slowly and steadily.

The PRE-1 specimen is shown in Fig. 7. Before the stress reached 17.30 MPa, the stress-strain change was approximately linear, and after that, the slope of the stress-strain curve decreased, and part of the cells in the interface and the mortar were damaged. With the damage and attenuation of elastic modulus, the strain increased at a faster speed. At this point, part of the cells failed. When the stress reached its peak value - 18.41 MPa, the specimen strength failed, and the strain increased at an even faster speed until the specimen failed.

4 Statistics of the failure surfaces of concrete specimens

According to the numerical simulation of the loading process, when the first principal strain of the interface and mortar cells reached the critical principal strain for failure εu, the strength of these cells failed, the damage variable D was 1, and the elastic modulus was completely damaged. After these cells were killed, with the load increasing, the interface cells were being transformed from the first phase of damage into the second phase and then from the second phase to being completely damaged, i.e., killed. In Step 10, the total number of killed cells was counted. Figure 8a and b list the number of killed cells during the loading process in Pull-1 and PRE-1, respectively.

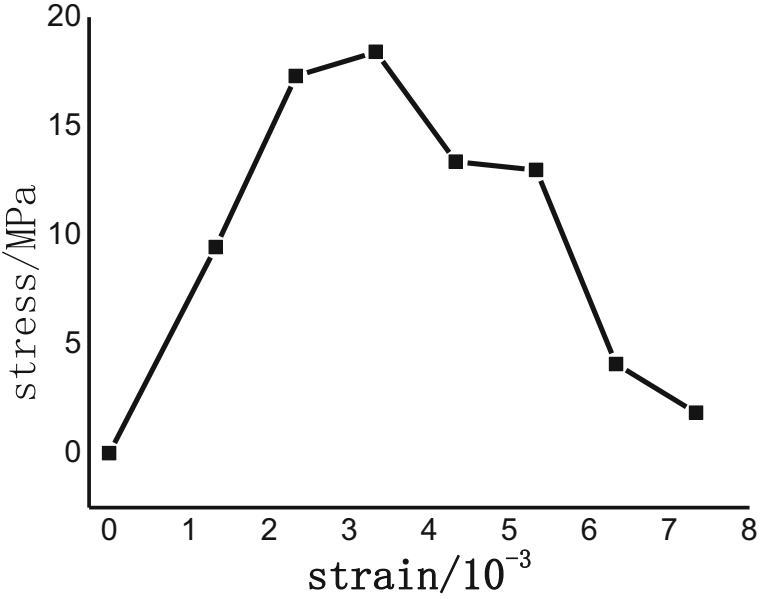

Fig. 7 PRE-1 stress-strain curve

By comparing the total number of killed cells in the interface and the mortar, the author found that the number of killed cells in the compression specimen was significantly higher than that in the tension specimen. With the increase of killed cells, cracks initiated. Due to the different numbers of killed cells in the mortar and the interface, the paths of crack development were also different.

5 Study of the energy consumption of load-bearing concrete specimens during the failure process

The strain energy of the interface cells and mortar cells at different positions on the same cross-section was analyzed respectively, as shown in Fig. 9a and b. As the displacement increased, the strain energy would always increase first and then decrease. The difference was that when the maximum strain was reached, the displacements were different. Both the interface and

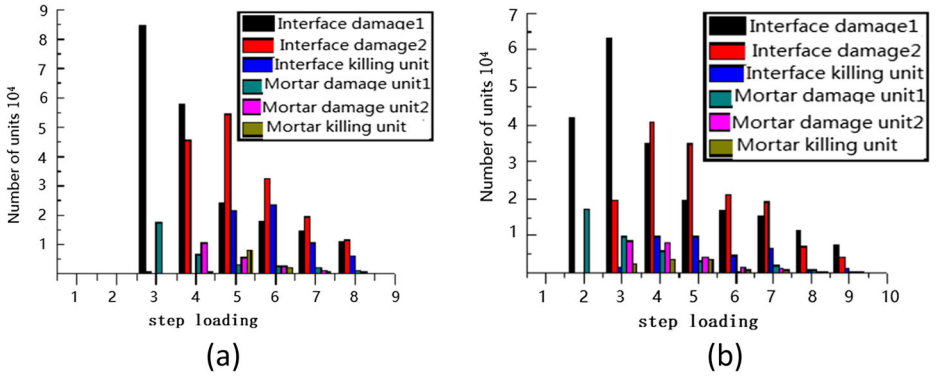

Fig. 8 **a** Number of killed cells in PRE-1 and **b** Number of killed cells in Pull-1

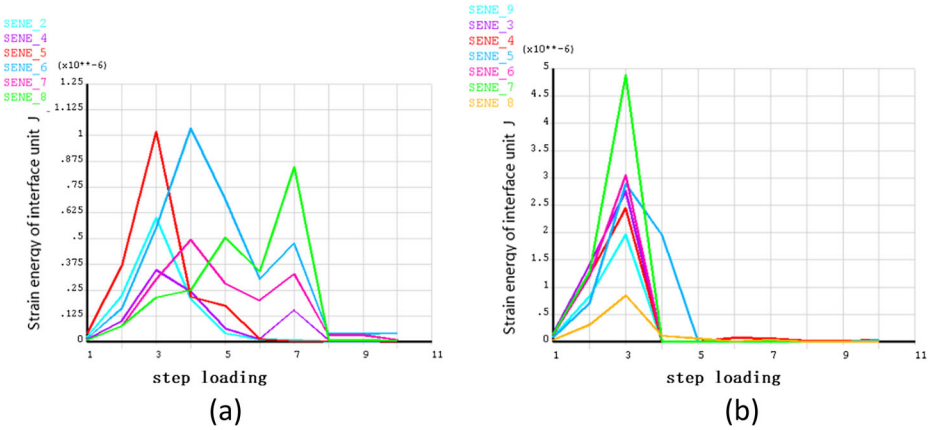

Fig.9 **a** Strain energy variation of interface cells and **b** Strain energy variation of mortar cells

mortar cells showed the same strain energy variation pattern. At the same loading step, the variation trends of strain energy were different and complex, showing that the strain energy of interface and mortar cells experienced a complex damage and consumption process under the effect of external force. With the damage of the elastic modulus, the energy consumption increased, and due to the different positions of the cells, as the displacement increased, the value of the stored elastic strain energy in each cell also varied, but the variation pattern of strain energy was consistent – the strain energy all increased in fluctuation to the extreme value and then the energy stored in each cell was fully released.

From Fig. 10a and b, it can be concluded that, as the elastic modulus of the cell decreased, the cells were continually damaged and eventually killed, and that the strain energy given from the outside to the interface was continuously lost. When killed cells started to appear, the cell strain energy started to be consumed, which was irrecoverable. As the number of killed cells increased, the resulting new surface continuously expanded, so did the energy loss.

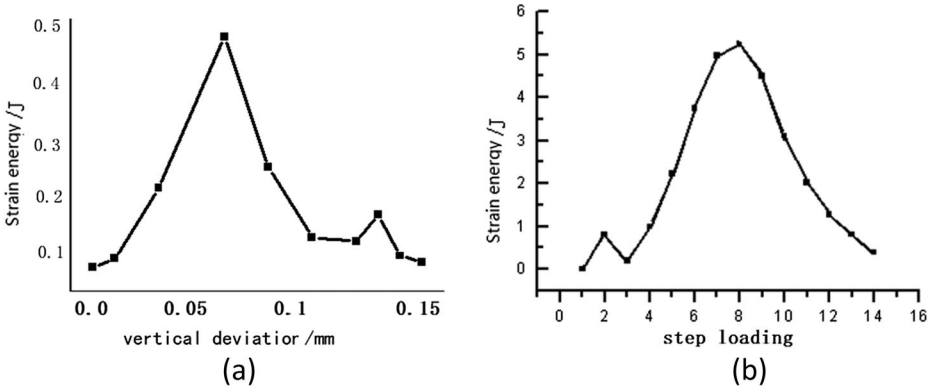

Fig.10 **a** Strain energy release curve of Pull-1 and **b** Strain energy release curve of PRE-1

6 Analysis of the crack evolution and strength of concrete specimens

The same patterns were obtained for compression and tension specimens as in the CT tests. Through analysis of the failure areas and strengths of the numerical test specimens Pre-1 and Pull-1, it was found that, the larger the failure area was in the specimen, the greater strength it had. This was because the different internal stress distributions in the different specimens caused the different damage variables of the elastic modulus, and due to different stress states, the initiation, development, expansion and penetration of microcracks into macrocracks showed different evolution patterns, leading to different failure forms and areas in different specimens and different amounts of energy consumed by the failure surfaces. All these finally caused the differences in strength. When specimens were subject to tensile and compressive forces respectively, the stress states inside the concrete materials were different, and the damage variables of the materials were also different, and what is more, the concrete itself was three-phase composite material, where the aggregate, mortar and interface had different bearing capacities, all of which lead to the differences in the initiation, development and penetration of cracks and even the whole failure process of the specimens. Both stress states can be divided into two parts – spheric stress and deviatoric stress tensors. In the case of tensile failure, the spheric stress component is positive and causes the development of microcracks together with the deviatoric stress component. However, when concrete is subject to shear compression and crushed, the spheric stress component is negative and the deviatoric stress causes the damage. Therefore, the elastic modulus follows different damage evolution rules when under compression and tension, respectively, causing different stresses on the materials and different crack initiation locations and development directions and further leading to different failure forms and failure areas and different energy storage capacities, i.e. the strengths of the materials.

7 Conclusion

For the concrete specimen subject to tension, its failure surface expanded along the one or two major cracks perpendicular to the principal tensile stress and caused instantaneous tensile failure, which was brittle failure. After the failure, the concrete specimens completely lost its tensile strength. According to the compression specimen test results, the failed specimen still had some residual strength and the failure area was large. During the compression process, the stress state was very complicated, and the failure surface developed along a number of cracks. The new surface formed after the failure was rough, with the debris falling off, and the specimen was damaged to a great extent. The numerical analysis and CT test of the concrete specimens fully prove that the tensile strength of concrete is an inherent property of the material, and a mechanical quantity that does not change with the external conditions. Usually, the measured strength is related to the stress state of the concrete specimen Under different stress states, cracks develop in different directions and paths in specimens, resulting in different extents of failures, i.e. different areas of crack surfaces.

Acknowledgements This paper is supported by Shaanxi Natural Science Youth Foundation of China (2017JQ5094) & Shaanxi Natural Science Foundation of China (2017JM5136).

References

1. Abrams DA (1917) Effect of rate of application of load on the compressive strength of concrete. ASTM J 17(part II):364–377
2. Bischoff PH, Perry SH (1991) Compressive behaviour of concrete at high strain rates. Mater Struct 24:425–450
3. Chen ZFS, Li QB (2008) Dynamic strength of concrete under biaxial stress. J Hydraul Eng 39(4):385–393
4. Deng Z, Sheng J, Wang Y (2019) Strength and constitutive model of recycled concrete under biaxial compression[J]. KSCE J Civ Eng 23(2):699–710
5. Khaliq W, Taimur (2018) Mechanical and physical response of recycled aggregates high-strength concrete at elevated temperatures[J]. Fire Saf J 96:203–214
6. Klepaczko JR, Brara A (2001) An experimental method for dynamic tensile testing of concrete by spa. International Journal of Impact Engineering 25:387–409
7. Liang XY, Dang FN, Tian W (2010) CT testing on fracture process of concrete under uniaxial compression. Journal of China Society 35:63–67
8. Liang XY, Dang FN, Tian W, Chen HQ (2010) Dynamic property influences and studies of concrete cylinder at different loading rates. Journal of Hydroelectric Engineering 31(9):35–40
9. Ma HF, Chen HQ, Li BK (2004) Review on micro-mechanics studies of concrete. Journal of China Institute of Water Resources and Hydropower Research 2(2):124–130
10. Ma HF, Chen HQ, Li BK (2005) Influence of meso-structure heterogeneity on dynamic bending strength of concrete. J Hydraul Eng 37(7):846–852
11. Malvar LJ, Ross CA (1998) Effects of strain rate on concrete strength. ACI Mater J 95:735–739
12. Morita M, Sasaki M (1989) Restart characteristics of turbofan engines. ISABE 89-7127, 9th, pp 1200–1206
13. Ottosen NS (1977) A failure criterion for concrete. J Eng Mech Div 103(4):527–535
14. Tedesco JW, Powell JC, Ross CA (1997) A strain-rate-dependent concrete material model for ADINA. Comput Struct 64(5–6):1053–1067
15. Tian W, Dang FN, Liu YW, Chen HQ (2008) Application of support vector machine to concrete CT image analysis. J Hydraul Eng 39(9):889–894
16. Vishalakshi KP, Revathi V, Reddy SS (2018) Effect of type of coarse aggregate on the strength properties and fracture energy of normal and high strength concrete[J]. Eng Fract Mech 194:52–60
17. Xinyu L, Faning D, Feng P, Hongmei T (2015) CT experimental study on concrete specimens based on the principle of minimum energy. Mater Res Innov 19(S5):1095–1101. p. 63–67

Xinyu Liang (1982-) , Female, Doctor, lecturer at Xi'an Technological university, the main research direction is numerical calculation of geotechnical engineering. E-mail: key_xinyu@163.com.